-Technical Paper-

TEMPERATURE DISTRIBUTION IN CRACKED MORTAR PRISM IN FIRE CONDITION

Mohammad M. RAOUF-FARD [*1], Atsuko TOMINAGA [*1], Minehiro NISHIYAMA [*2], Masanobu SAKASHITA [*3]

ABSTRACT

A series of fire tests on reinforced concrete (RC) members have been conducted to study the structural response of different parts exposed to elevated temperatures. However, the effect of crack had not been investigated fully yet. Since cracks make the entire RC structure susceptible to fire, the present paper studies effect of cracks on internal temperature distributions by conducting a series of fire tests on mortar prism specimens along with FEM analyses. The cracked zone tended to attain higher internal temperatures than its adjacent intact zones.

Keywords: reinforced concrete, mortar, elevated temperatures, crack, fire test, temperature distribution

1. INTRODUCTION

Concrete structures have a good reputation for anti-fire resistant ability. This is because of a non-combustible material called concrete, which has a low thermal conductivity. The cement paste in concrete undergoes an endothermic reaction when heated, which assists in reducing the temperature rise in fire-exposed concrete structures [1]. Since 2010, the authors have conducted a series of fire tests on reinforced concrete (RC) members and frames subjected to service loads to study the structural response of different parts exposed to elevated temperature[2, 3]. However, the effect of crack had not been investigated yet. Since widening of existing cracks and formation of new cracks due to an earthquake or the aging process, make the entire frame susceptible to fires, the authors have investigated the effect of cracks on temperature distribution within RC members in fire conditions.

The purpose of this research was to understand whether crack has any significant effect on temperature distribution within the fire-exposed members, and if it does, to what extent. To achieve this, twenty three small sized prisms made of different materials such as concrete, mortar, and cement paste were designed in the first step. The experimental parameter was crack width: 0mm, 0.3mm, and 5mm. All the specimens were instrumented with several thermocouples at different cross-sections to measure the internal temperatures at different locations close to the cracked zone. Several other thermocouples were installed at different locations around the specimens and inside the furnace. Later the data was put directly into the finite element models. Prism specimens were exposed to fire only from one face in which the artificial crack opening was located. Other five sides of the prisms where sufficiently thermally insulated. The small scale furnace and some uncertainties made us conduct a series of pilot tests. However, the details of the pilot tests are not reported in this literature. Based on the results of the pilot tests, twelve 45×50×150mm mortar prism specimens were made.

Also a series of nonlinear finite element (FE) models were developed via FE modelling program FINAL [4]. The measured temperatures and the thermal nonlinearity of materials have been directly inserted into the models to verify the temperature distribution patterns against the tests.

2. EXPERIMENTAL WORK

2.1. Specimens preparation

Due to the small size of the furnace and the uncertainties in the specimens' dimensions, cracks' conditions, number and location of the thermocouples, and the casted material, several pilot specimens were built and tested to introduce the most appropriate test plan. Eleven pilot specimens in various dimensions and materials and also different thermocouple arrangements were built and underwent fire test. By analyzing the results, twelve 45×50×150mm mortar prisms were manufactured as the real test specimens. To ease the mix compaction in the thermocouple-dense narrow space and also to prevent course aggregate placement in between any two thermocouples, mortar was used. Fig. 1 shows the specimens geometry details. Table 1 and 2 show the mix portion properties and the specimens details, respectively. All the faces of each prism except the crack-opening face were covered with thermal insulator sheets.

*1 Graduate School of Engineering, Kyoto University, JCI Student Member
*2 Professor, Dept. of Structural and Architectural Engineering, Kyoto University, JCI Member
*3 Assistant Prof., Dept. of Structural and Architectural Engineering, Kyoto University, JCI Member

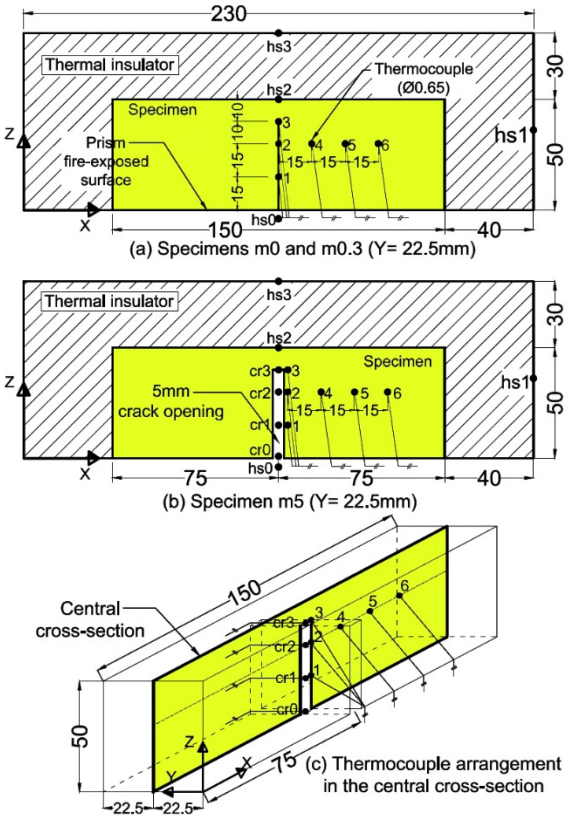

Fig. 1 Dimensions and details of specimens (mm): hs0 and cr0 are located at the crack-opening face, z=0mm and z=2mm, respectively.

Table 1 Mortar mix properties

Mix proportion (kg/m^3)			w/c ratio (%)	Moisture content (%)
Cement	Water	Sand		
584	292	1753	50	7.58

Table 2 Crack width and number of specimens

Specimen	material	crack width (mm)	number
m0	mortar	0.0	4
m0.3	mortar	0.3	4
m5	mortar	5.0	4

2.2. Fire test

The specimens' placement is schematically illustrated in Fig. 2. The furnace was set according to the standard fire ISO834 in Fig. 3 and the test duration was 120 minutes. Table 3 shows the order of the tests.

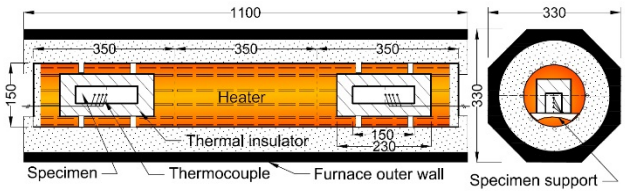

Fig. 2 Test furnace and schematic placement of specimens (unit: mm)

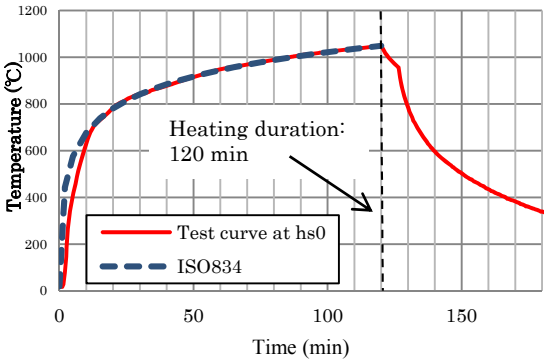

Fig. 3 Standard temperature-time curve ISO834 and the measured one of m5(3) at hs0

Table 3 Tests' order

Test Number	Specimen	
Test 1	m0(1)	m5(1)
Test 2	m0(2)	m5(2)
Test 3	m0(3)	m5(3)
Test 4	m0(4)	m5(4)
Test 5	m0.3(1)	m0.3(2)
Test 6	m0.3(3)	m0.3(4)

2.3. Fire tests and results

(1) Specimen condition

Since there was no observation window on the furnace, the visual inspection of specimens was not possible. However, in each test, as soon as the heating process finished, by removing the furnace lid the in-place inspection was done. While specimens were cooling down to the room temperature, due to the thermal differences some major cracks formed. Fig. 4 shows specimen m5(3) together with its external thermocouples after it was cooled down. Mortar spalling and thermal cracks were seen in all the specimens similarly.

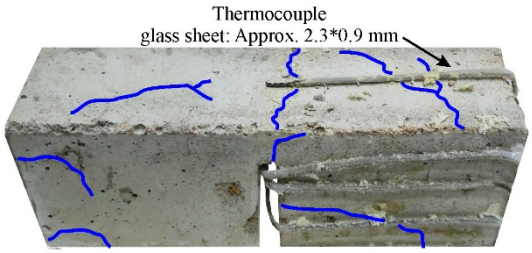

Fig. 4 Specimen m5(3), 2 hours after the fire test (blue line: thermal cracks)

(2) External temperature distribution

As can be seen in Fig. 5, the furnace thermal distribution was not quite equivalent; however, the target fire-exposed surface at each test received appropriate standard heat, i.e., the thermocouple hs0 located at the heating surface of each specimen except the very first minutes of the tests, correctly followed the ISO834 temperature curve.

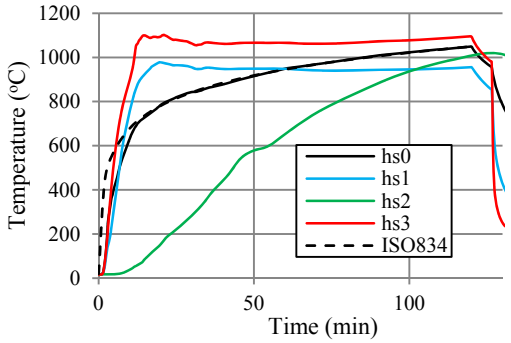

Fig. 5 External temperatures of m5(3)

(3) Internal temperature distribution

Due to the small dimensions of specimens, almost after 90 minutes the internal temperatures of thermocouples 2 to 6 reached roughly the same values. However, thermocouple 1, the closest to the heating surface recorded higher temperatures of all. Fig. 6 shows the temperature distributions of m5(3). Thermal differences between locations 2, 4, 5, and 6 were slightly varying through the test. The details are discussed later in this section.

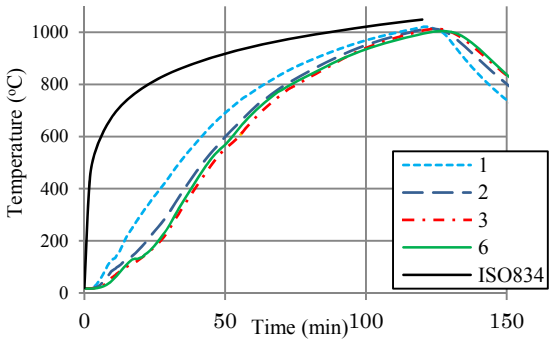

Fig. 6 Internal temperature distribution of m5(3)

(4) Temperature distribution inside the crack of m3(3)

Thermocouples cr1, cr2, and cr3 were aligned to thermocouples 1, 2, and 3, respectively. Thermocouple cr0 was just at the opening of the crack. Fig. 7 shows the temperatures inside the crack of m5(3) against the crack face .

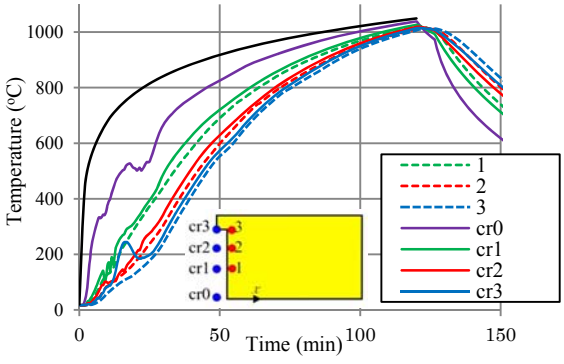

Fig. 7 Temperature distribution of m5(3)'s crack

It is assumed that heated air circulation inside the crack led to some thermal fluctuations within the first 30 minutes of the tests. The overall air temperatures inside the cracks at different elevations were higher than the immediate locations inside the specimens. However, the mechanism of heat convention of the entrapped air inside narrow cracks should be investigated more.

(5) Comparison between temperatures of 2, 4, 5, and 6

The measure of the destructive impact of a fire which is called fire severity is mainly dependent on the level and duration of the high temperature. In this test, in order to provide equivalent fire severity, the standard fire ISO834 was used. To conduct a comparison between the specimens' internal temperatures at locations 2, 4, 5, and 6, the average temperatures based on ISO834 temperature time interval of 30 minutes were acquired and plotted in Fig. 8. The average temperatures of cr2 are plotted in the figures as well. As can be seen in the figures, in the first 30 minutes the average values show an inverse order. That is, m0 looks hotter than m0.3 and m5 and also m0.3 looks hotter than m5. This is because of a larger variance of temperature values recorded in the first 30 minutes.

Fig. 9 and 10 show internal temperature differences between the cracked specimens (m0.3 and m5) and non-cracked one (m0) at locations 2, 4, 5, and 6. As can be seen in the figures, the cracked specimens m0.3 and m5 tended to absorb more heat than m0. However, the temperature discrepancy values between the specimens varied as the fire test proceeded. In 30 minutes, the thermal difference values were fluctuating. This could be because of the initial instability in air circulation inside the crack opening. Table 4 shows temperature differences of the cracked specimens against the non-cracked one (m0). According to the test results, except for the first 30 minutes, the crack faces of m0.3 and m5 were clearly hotter than their nearby locations inside the specimens. It proved the effect of crack on the internal thermal distribution of the cracked prisms. As the fire continued the cracked zone showed more uniform thermal distribution. As can be seen in Table 4, the maximum temperature discrepancies occurred in 60 minutes

Table 4 Internal temperature difference between cracked specimens and m0 at locations 2, 4, 5, and 6

	m0			
	ΔT^{*}_{30min}	ΔT_{60min}	ΔT_{90min}	ΔT_{120min}
m0.3	-14～16	19～32	14～20	7～11
m5.0	-22～-2	29～50	19～31	8～21

*Temperature unit: degrees Celsius

*ΔT is the average temperature of each cracked specimen minus the average temperature of specimen m0

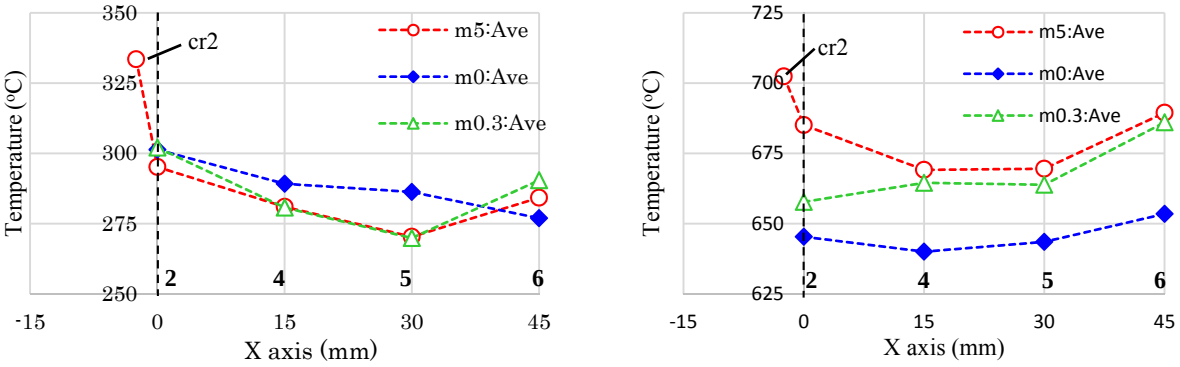

(a) 30 minutes (b) 60 minutes

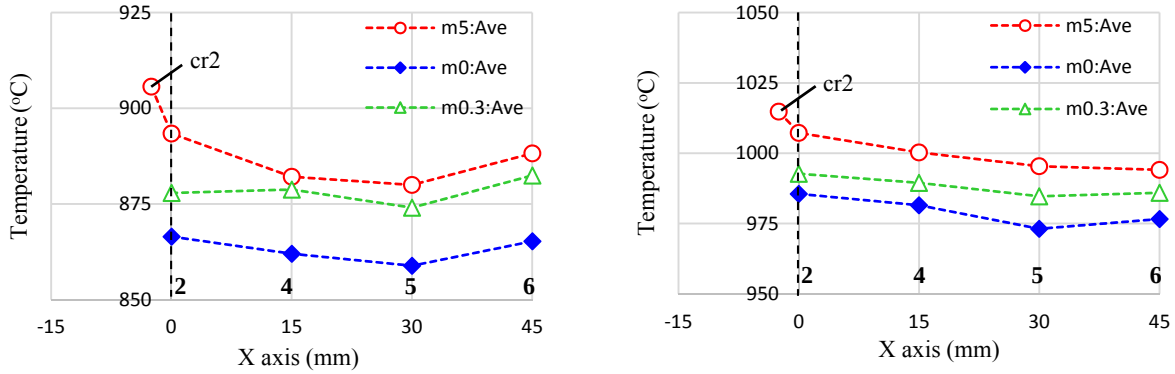

(c) 90 minutes (d) 120 minutes

Fig. 8 Average temperatures at different time stages

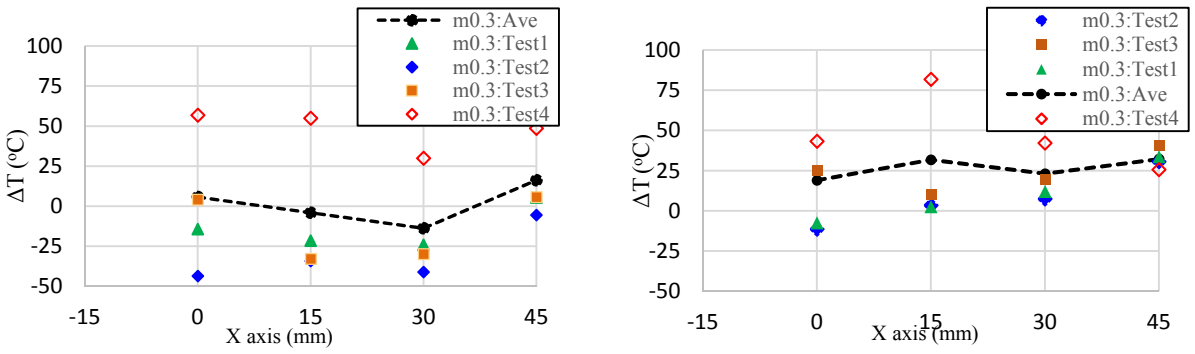

(a) 30 minutes (b) 60 minutes

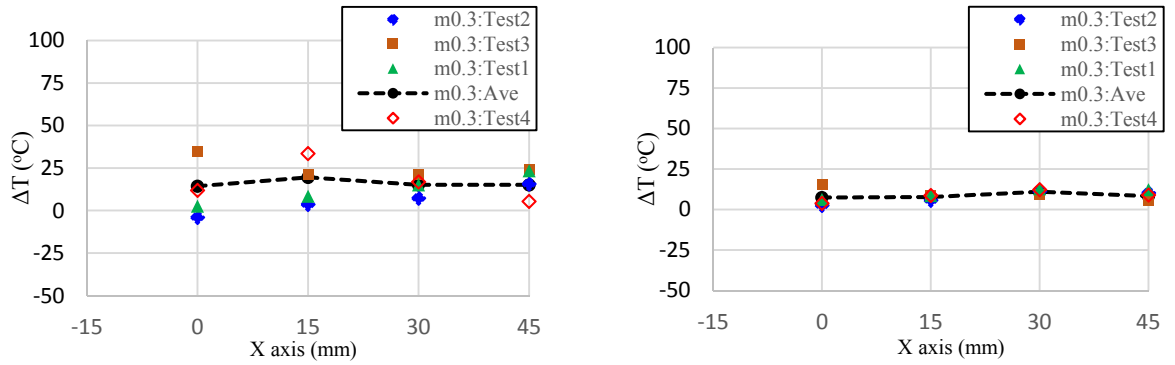

(c) 90 minutes (d) 120 minutes

Fig. 9 Internal temperature differences between m0.3 and m0 at different time stages

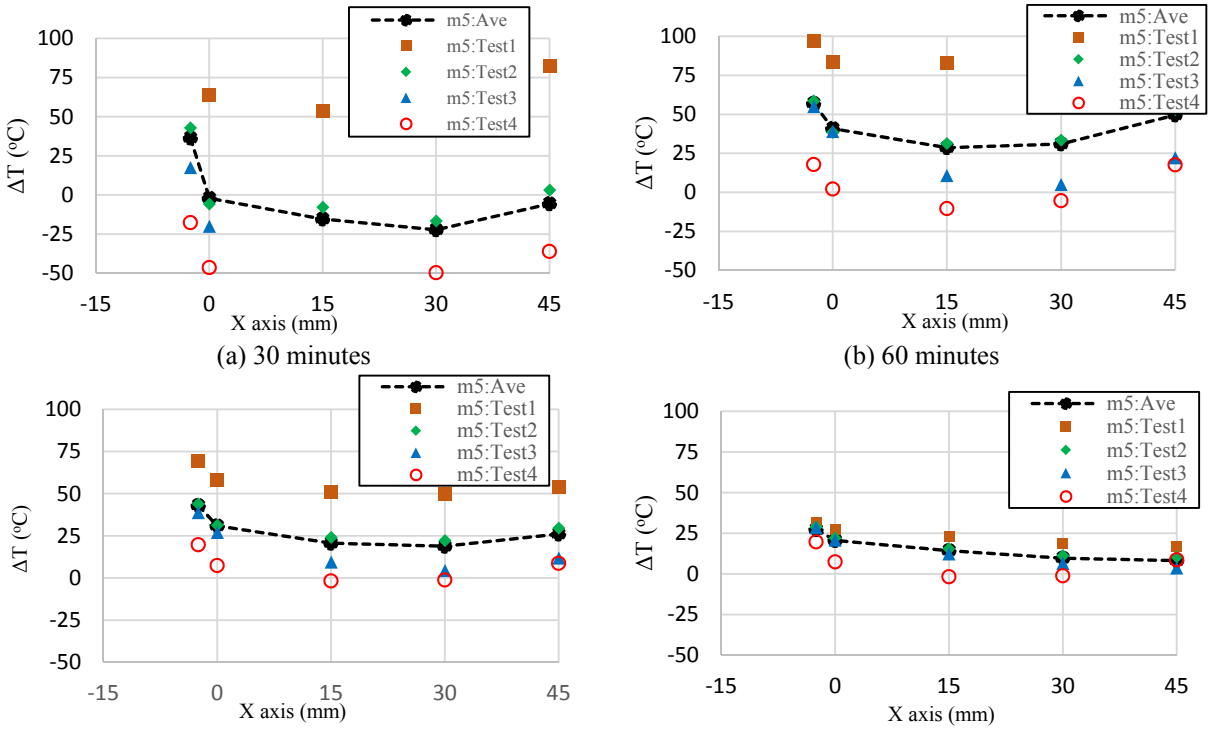

(a) 30 minutes (b) 60 minutes

(c) 90 minutes (d) 120 minutes

Fig. 10 Internal temperature differences between m5 and m0 at different time stages

3. NONLINAR FINITE ELEMENT ANALYSIS

To conduct a numerical thermal analysis of the test, FEM analysis software FINAL [4] was used. Crank-Nicolson method [5] was chosen for solving the heat equations considering the constant β=0.5 and the lumped heat-capacity ratio=1.

3.1. Finite element modeling

Fig. 11 illustrates the Z-X and Z-Y cross sections of the full 3D mesh. All the elements are hexahedral. Specimen m0 and m5 were analyzed in this step.

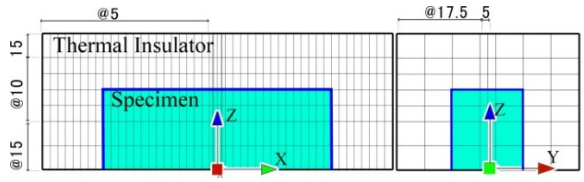

Fig.11 FE mesh of the specimens (mm)

3.2. Thermal characteristics of materials

Table 5 and 6 show the time-dependent characteristics of insulator and mortar, respectively.

Table 5 Thermal characteristics of insulator*

Temperature (°C)	Thermal conductivity (W/m.K)	Temperature (°C)	Thermal conductivity (W/m.K)
20	0.02000	200	0.04009
100	0.02009	300	0.06009

*Specific heat= 0.25(kJ/kg.K); Density=130(kg/m^3)

Table 6 Thermal characteristics of mortar

Temp. (°C)	Thermal conductivity* (W/m.K)	Spec. heat capacity** (kJ/kg.K)	Density** (kg/m^3)
50	0.47	0.142	1055
250	0.62	0.213	1002
450	0.52	0.272	976
750	0.57	0.342	949
800	0.58	0.351	949

*According to Harada[6]

**AIJ guidebook for fire-resistive performance of structural materials [7]

3.3. Analysis results

Fig. 12 shows the FE result of Test 3 for m0 and m5 at location 2. FE analysis shows that the cracked specimen m5 tended to absorb more heat in location 2 than the non-cracked m0.

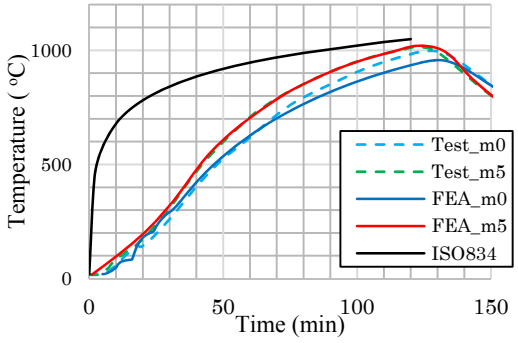

Fig. 12 Temperature distribution at location 2

Fig. 13 and 14 illustrate the thermal gradients of m0 and m5 at different time stages, respectively.

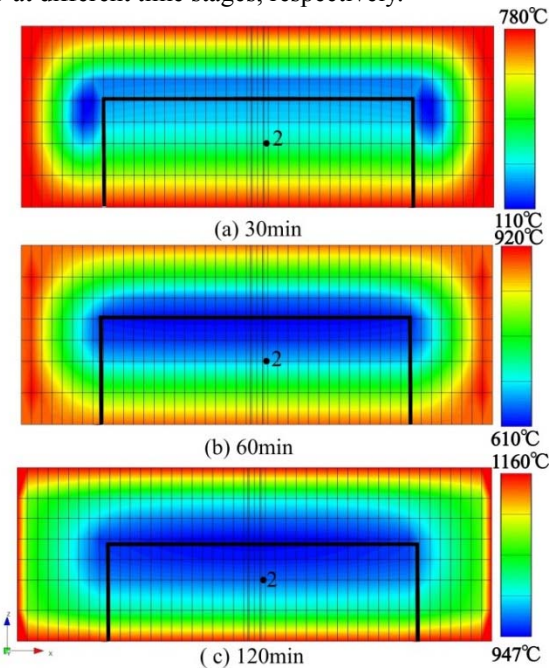

Fig. 13 Thermal contours of m0

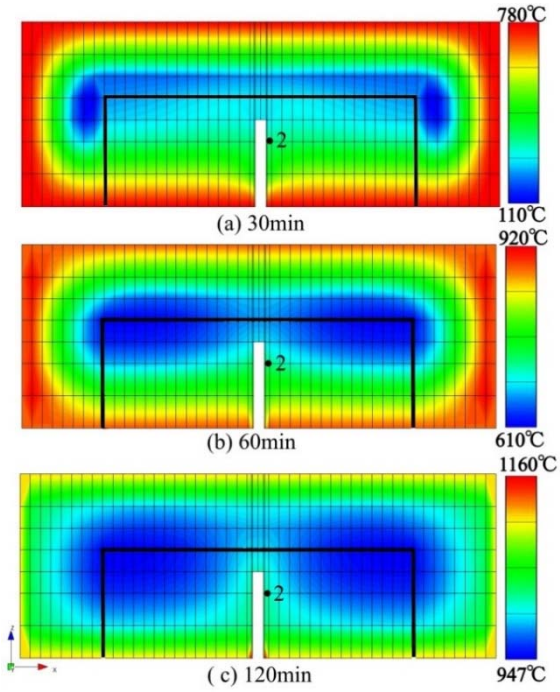

Fig. 14 Thermal contours of m5

The FE thermal contours of m0 and m5 clearly show the temperature distribution patterns within the specimens. The non-cracked specimen (m0) has horizontal parallel thermal contours; however, the cracked one (m5) has parabolic contours, especially in the cracked zone. These two thermal gradient patterns declared the existence of thermal difference between the cracked and non-cracked specimens.

4. CONCLUSIONS

To investigate the effect of cracks on thermal distribution within concrete members a series of experimental studies along with nonlinear finite element analyses were conducted on twelve mortar prisms. The following conclusions can be drawn:

(1) 0.3mm-crack specimens during the fire test compared with the non-cracked ones attained higher internal temperatures to maximum of 32°C.
(2) 5mm-crack specimens compared with the non-cracked ones attained higher internal temperatures to maximum of 50°C.
(3) The heat convection mechanism of the trapped air in the crack should be investigated to figure out the reason of scattered data within the first 30 minutes of the fire test.
(4) Based on FE results, temperature distributions within the non-cracked specimens were almost linear and parallel to the fire-exposed surface. However, the cracked ones tended to have parabolic temperature contours along the cracked zone.
(5) In reality roughness of crack face and its direction, stress condition, and fire regime may lead to different readings. Therefore, the authors have conducted a series of fire tests on cracked RC members to verify the understandings. The results will be published elsewhere.

ACKNOWLEDGEMENT

This research work was financially supported by JSPS KAKENHI Grant Number 2324610.

REFERENCES

[1] Buchanan, A., “Structural Design for Fire Safety”, John Willey & Sons Inc., 2001, p 225
[2] Nishiyama, M., “Fire-Resistance Tests on Reinforced Concrete External Beam-Column Subassemblages”, J. Struct. Constr. Eng. Trans. AIJ, 2012, pp 209-210 (in Japanese)
[3] Lim, S., “Fire-Resistance Tests on statically indeterminate Reinforced Concrete Frame”, J. Struct. Constr. Eng. Trans. AIJ, 2011, pp 25-26 (in Japanese)
[4] ITOCHU Corporation, FINAL/V11.
[5] Crank, J.; Nicolson, P., "A practical method for numerical evaluation of solutions of partial differential equations of the heat conduction type". Proc. Camb. Phil. Soc. 43 (1), pp 50–67.
[6] Harada, T., “ Variation of Thermal Diffusivity of Cement-Mortar and Concrete at High Temperatures”, Journal of Structural and Construction Engineering, AIJ, Mar. 1958, pp. 7-13. (in Japanese)
[7] Architectural Institute of Japan, “Guidebook for fire-resistive performance of structural materials”, 2009, p38 (in Japanese)